Journal of Molecular Liquids 310 (2020) 113044

Contents lists available at ScienceDirect

Journal of Molecular Liquids

journal homepage: www.elsevier.com/locate/molliq

The cation effect on the solubility of glycylglycine and N-acetylglycine in aqueous solution: Experimental and molecular dynamics studies

Germán Pérez-Sánchez [a], Yoselyn S. Santos [b], Olga Ferreira [b,c], João A.P. Coutinho [a], José R.B. Gomes [a], Simão P. Pinho [b,c,*]

[a] CICECO — Aveiro Institute of Materials, Department of Chemistry, University of Aveiro, 3810-193 Aveiro, Portugal
[b] Centro de Investigação de Montanha (CIMO), Instituto Politécnico de Bragança, Campus de Santa Apolónia, 5300-253 Bragança, Portugal
[c] Laboratory of Separation and Reaction Engineering - Laboratory of Catalysis and Materials (LSRE-LCM), Instituto Politécnico de Bragança, Campus de Santa Apolónia, 5300-253 Bragança, Portugal

ARTICLE INFO

Article history:
Received 27 November 2019
Received in revised form 29 March 2020
Accepted 31 March 2020
Available online 21 April 2020

Keywords:
Salt effects
Solubility
Glycine derivatives
Experimental
Molecular dynamics

ABSTRACT

The specific interactions of ions with biomolecules in aqueous solutions play a very important role in the life sciences and biotechnology. This work aims to study the effect of NaCl, KCl, NH_4Cl, $CaCl_2$ or $MgCl_2$ on the solubility of two glycine derivatives, glycylglycine (a.k.a. diglycine) and *N*-acetylglycine, and to understand the nature of the interactions present on these systems. Experimentally, upon increasing the concentration of the salts, the solubility of *N*-acetylglycine decreased while the solubility of diglycine increased, with divalent cations inducing a greater salting-in on the solubility of diglycine than monovalent cations. For diglycine, the results from molecular dynamics simulations correlate well with the salting-in effect with interactions involving the cation and the carboxylate group, while for neutral *N*-acetylglycine the interactions between the chloride anion and the hydrogen atom of the carboxylic acid group, and between the carbonyl group of the peptide bond and the cation, can be exploited to describe the generalized salting-out effect.

1. Introduction

The understanding of the molecular-level mechanisms that govern the solubility, stability and activity of proteins in the presence of salts is of utmost importance from a biological and pharmaceutical point of view, as electrolyte solutions are the natural environment of such essential biomolecules. Nevertheless, the direct study of protein/salt solutions is complex, suggesting the use of model compounds of increasing degree of complexity. A few studies have been published in this area, most focusing on model compounds such as amino acids and derivatives. In that context, we have studied the solubility of several amino acids in aqueous solutions containing inorganic salts [1–5]. For peptides, this type of experimental data is much scarcer. Earlier work carried out in the seventies of the last century about the effect of salts on peptides included the measurement of the solubility of acetyltetraglycine ethyl ester [6], *N*-acetylamino acids ethyl esters with hydrocarbon side chains [7] and *N*-acetylethyl esters of glycine, diglycine and triglycine [8]. However, the conclusions of these pioneering works might have been affected by the partially unsuccessful synthesis of the oligoglycines, as discussed by Paterová et al. [9].

A few more recent studies can also be found in the literature regarding the solubility of glycine and its oligopeptides, in particular, glycine, diglycine, and triglycine in aqueous solutions of $NaNO_3$ [10]; diglycine and glycyl-L-alanine in aqueous solutions of NaCl, Na_2SO_4 or $(NH_4)_2SO_4$ [11]; a series of oligoglycines from diglycine to hexaglycine in aqueous solutions of NaCl and NaOH [12]; and glycine, diglycine, triglycine, tetraglycine, and cyclic glycylglycine in KCl, KBr and KCH_3COO [13].

A recent and interesting work [9] discusses the use of NMR techniques to understand the relative positioning of the ions by monitoring the protons of the three methylene units of capped and uncapped triglycine, showing that "the Hofmeister series for anions changed from a direct to a reversed series upon uncapping the N-terminus", concluding that ion effects on the peptide functional groups have a key contribution to the physical properties of the system.

Molecular dynamics (MD) simulations also played a very important role to understand, at the molecular level, the experimentally observed behaviour of the peptides in aqueous saline solutions. Although models for amino acids are well established [14,15], the representation of the peptide bond requires a careful step by step approach. In the recent literature, similar studies are being pursued to model different peptides

* Corresponding author at: Centro de Investigação de Montanha (CIMO), Instituto Politécnico de Bragança, Campus de Santa Apolónia, 5300-253 Bragança, Portugal.
E-mail address: spinho@ipb.pt (S.P. Pinho).

https://doi.org/10.1016/j.molliq.2020.113044
0167-7322/

such as, for example: diglycine dipeptide with transition metal ions in aqueous solutions [16]; alanine dipeptide in water [17]; urea or glycine betaine, and triglycine in aqueous solutions [18]; capped and uncapped triglycine in water, with NaSCN, NaI, NaCl, NaBr or sodium sulfate [9].

In order to extend the body of knowledge on the interaction of biomolecules with ions in aqueous solutions, more complex molecules than amino acids [19,20], presenting the peptide bond, are here studied. These can also contribute to better assess the relative importance of the peptide bond in the interaction with ions in aqueous solutions, which is under strong scientific debate. Therefore, here the measurement of the solubility of diglycine or *N*-acetyl glycine in aqueous solutions containing KCl, NaCl, NH_4Cl, $CaCl_2$ or $MgCl_2$, at the temperature of 298.2 K are carried out. The cations were selected for covering a wide range of aqueous solubility effects, considering the Hofmeister [21] series of ions. Besides that, a computational model for classical MD simulations for elucidating the molecular-level interactions in these complex solutions is also considered.

2. Experimental part

2.1. Solubility measurements

2.1.1. Materials

The source and purity of the compounds used in this work are described in Table 1. All chemicals were used as received and, excluding the hydrated salts, the solids were kept in a dehydrator with silica gel to avoid water contamination. In all experiments, double-ionized water was used. The water content of the hydrated salts was measured by dissolving a certain mass of salt in methanol, which was followed by titration of the solution using the Karl-Fisher method (Metrohm model 736 GP Titrino), with an uncertainty at a 95% confidence interval better than 0.4% in mass percentage.

2.1.2. Experimental procedure

The experiments were carried out at 298.2 K, using the analytical isothermal shake-flask method, as described previously in detail [5]. Saturated solutions were prepared by mixing a small excess of solid solute with about 80 cm^3 of solvent, already prepared by weighing ($\pm$ 0.1 mg) the appropriate amounts of salt and water. Then, the solution was continuously stirred for 48 h and, after, allowed to settle during at least 12 h before sampling. The temperature was monitored with four-wire platinum resistance probes (Pt-104, Pico-Technology), with accuracy $\pm$0.1 K.

At least three samples of about 5 cm^3 of the saturated liquid phase were collected using previously heated plastic syringes coupled with polypropylene filters (0.45 μm). The quantitative analysis of the composition of the saturated solutions was performed by gravimetry (anhydrous salts) or by measuring the refractive index (hydrated salts).

For the gravimetric method, the samples were placed into preweighed ($\pm$0.1 mg) glass vessels and immediately weighed. Then, all the solvent was evaporated, and the crystals dried completely in a drying stove at 343.15 K for 3 days. Finally, the glass vessels were cooled in a dehydrator with silica gel for one day and weighed. The process was regularly repeated until a constant mass was achieved.

For aqueous solutions containing hydrated salts, refraction index measurements were performed using a digital refractometer (Abbemat 500, Anton Paar) with a reproducibility within 2×10^{-5} and temperature accuracy and stability better than $\pm$0.03 K. Firstly, the calibration curve was built ($r^2 > 0.999$), relating the biomolecule concentration (in g/kg of water) with the refraction index measured in aqueous salt solutions at fixed salt molality in six standard solutions of known biomolecule concentration. The collected samples were diluted with a weighed amount of binary salt aqueous solution at the same salt molality as the ternary saturated solution. After mixing, the refraction index was measured following standard procedures, and the solubility calculated.

The pH of the saturated solutions was also measured at 298.2 K (pH meter inoLab pH 720, WTW).

2.2. Computational methods

Classical molecular dynamics (MD) simulations were carried out in the NpT isothermal-isobaric ensemble, at a temperature of 298.2 K and a pressure of 1 bar, with the Gromacs 4.5 computer code [15]. The temperature and pressure were fixed with the Nosé-Hoover thermostat [22,23] and the Parrinello-Rahman barostat [24], respectively. The leap-frog algorithm [25] was used to integrate the equations of motion with a time step of 2 fs.

All the simulations started with all the molecules at random positions in cubic boxes with an average size of 32 Å in which periodic boundary conditions were applied in three dimensions. Diglycine and N-acetyglycine water solutions were prepared with 20 diglycine and 6 *N*-acetylglycine species solvated by 1000 water molecules. The diglycine molecule was modeled in its zwitterionic form. In the case of *N*-acetylglycine, simulations were performed for the neutral and also for a 50–50% mixture of deprotonated and neutral forms for exploring the effect of pH. The concentration of the $CaCl_2$, KCl, $MgCl_2$, NaCl and NH_4Cl salts added to the aqueous diglycine and *N*-acetylglycine solutions was 2.0 M, which corresponds to insertion in the simulation boxes of 36 cations and 36 (or 72) chloride anions in the case of singly- (or doubly-) charged cations. For comparison purposes, similar simulations were also performed for the amino acid glycine (20 glycine species solvated by 1000 water molecules). The same computational protocol was used for all the molecular systems considered in this work: first, an energy minimization with the steepest descent algorithm was performed to prevent short-range contacts between atoms, which was followed by short equilibration runs in the NVT and then NpT ensembles followed by 10 ns of an NpT production run. The total energy, temperature and density were checked in each run to ensure that the equilibrium was attained.

Table 1
Pure component source and purity.

Compound	Chemical formula	Source	Mass purity (%)
Diglycine (glycylglycine)	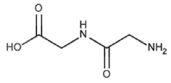	Acros Organics	99.0
N-acetylglycine	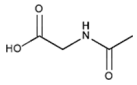	Acros Organics	99.0
Methanol	CH_3OH	Carlo Erba	99.9
Ammonium chloride	NH_4Cl	Panreac	99.5
Calcium chloride	$CaCl_2.2H_2O$	Panreac	99.0–105.0
Magnesium chloride	$MgCl_2.6H_2O$	Panreac	99.0
Potassium chloride	KCl	Merck	99.0
Sodium chloride	NaCl	Merck	99.5

The energy contributions in the potential energy function were bond stretching, angle bending, torsion, Lennard−Jones (LJ) and Coulombic terms. A cut-off of 1.2 nm in LJ potential was employed while long-range electrostatic interactions were evaluated with the particle mesh Ewald method (PME) [26] with a cutoff radius of 1.2 nm. Bond lengths were constrained by the LINCS algorithm [27] whereas angle bending was modeled by a harmonic potential and the dihedral torsion by a Ryckaert-Bellemans function. Rigid SPC/E potential [28] was used to represent the water molecules, whereas the OPLS all-atom potential [29–31] was used for diglycine, *N*-acetylglycine, glycine and the salts.

The force field choice is of utmost importance to study thermodynamic properties through computer simulations. Previously, the OPLS force field was found to provide good results for aqueous-saline solutions of different amino acids systems [4,5,19]. Despite some small differences found in the absolute degrees of binding when considering different non-polarizable force fields, the relative changes along the Hofmeister series remained unchanged [19]. It was also found that non-polarizable and polarizable models lead to the same qualitative description of the interaction between the halides and the basic amino acids arginine, histidine and lysine in water [32].

3. Results and discussion

3.1. Experimental solubility data

The measured values of the solubility of diglycine and *N*-acetylglycine in pure water and in the aqueous solutions of NaCl, KCl, NH_4Cl, $CaCl_2$ and $MgCl_2$, at $T = 298.2$ K, are presented in Tables 2 and 3, respectively, together with the correspondent standard deviation. The maximum coefficient of variation is 0.38% for the systems containing diglycine and 1.41% for *N*-acetylglycine solutions. The pH values of the saturated solutions are also presented. For diglycine, the pH ranged between 5.1 and 5.7 and, under these conditions, diglycine presents both positive (ammonium group, NH_3^+) and negative charges (carboxylate group, COO^-), i.e. zwitterionic behaviour. For *N*-acetylglycine, the pH varied between 1.1 and 3.1, which results in a high proportion of the neutral form of this biomolecule in the studied electrolyte solutions. The distribution of the chemical species as a function of pH is presented in supporting information (Fig. S1).

As mentioned before, the experimental solubility data available in the literature for these systems is scarce. In particular, for *N*-acetylglycine no information is available even for its solubility in pure water at 298.2 K. The solubility of diglycine in pure water measured in this work (228.0 g/kg water) is in good agreement with the average solubility from three independent sources [10,11,13], which is 228.03 g/kg of water, supporting the quality of the data measured in this work. Concerning the salt effect, Fig. S2 shows that the solubility data measured in this work are in agreement with the results from the literature [11], as both sets show a similar salting-in effect on the solubility of diglycine, upon addition of NaCl.

Table 2
Diglycine solubility (g/kg of water, relative uncertainty better than $u_r(S) = 0.01$) at 298.2 K as a function of salt molality.

Salt	Salt molality	Solubility (g/kg of water)	Standard deviation (g/kg of water)	pH
–	0.00	228.0	0.10	[a]
NaCl	0.49	242.9	0.42	5.7
	1.00	252.1	0.48	5.7
	2.01	265.1	0.36	5.7
KCl	0.50	241.4	0.15	[a]
	1.00	248.9	0.10	[a]
	2.00	254.4	0.96	[a]
NH_4Cl	0.50	244.6	0.11	[a]
	1.00	255.3	0.05	[a]
	2.00	266.4	0.22	[a]
$CaCl_2$	0.50	305.7	0.42	5.6
	1.00	371.2	0.49	5.5
	2.00	513.9	0.73	5.2
$MgCl_2$	0.50	280.6	0.17	5.5
	1.00	320.1	0.88	5.4
	2.00	365.3	0.28	5.1

[a] Not measured.

Table 3
N-acetylglycine solubility (g/kg of water, relative uncertainty better than $u_r(S) = 0.02$) at 298.2 K as a function of salt molality.

Salt	Salt molality	Solubility (g/kg of water)	Standard deviation (g/kg of water)	pH
–	0.00	41.4	0.45	–[a]
NaCl	0.50	37.9	0.25	3.0
	1.00	34.7	0.05	3.1
	2.00	29.0	0.12	3.1
KCl	0.50	39.8	0.10	2.1
	1.00	37.3	0.23	2.0
	2.00	34.4	0.14	2.0
NH_4Cl	0.50	40.1	0.12	2.0
	1.00	38.1	0.10	1.9
	2.00	34.9	0.49	–[a]
$CaCl_2$	0.50	36.7	0.08	1.7
	1.00	32.8	0.05	1.5
	2.00	25.8	0.23	1.1
$MgCl_2$	0.50	36.0	0.01	1.8
	1.00	29.8	0.04	1.6
	2.00	26.8	0.31	1.2

[a] Not measured.

Fig. 1 shows the relative solubility of the glycine derivatives and, for comparison purposes, alanine in the aqueous solutions containing salts studied in this work. The remarkable impact of the salts containing divalent cations on the increase of diglycine solubility should be here highlighted. The data for alanine were taken from the literature [1,4,5,33].

The salting-in effect in diglycine is noticeable in chloride salts where $K^+ \approx Na^+ \approx NH_4^+ < Mg^{2+} < Ca^{2+}$. The effect of the strongly hydrated divalent cations Mg^{2+} or Ca^{2+} on the solubility of different amino acids (alanine, valine and isoleucine) was studied before [4,5]. MD studies suggested that those cations do not establish important (direct) interactions with the hydrophobic parts of the amino acids, but, due to their high charge density, they were able to form charged complexes with the biomolecules, which are very soluble, promoting thus strong increases of their aqueous solubilities [4,5]. As expected, a similar behaviour for diglycine is observed mainly due to the preferential zwitterionic form of the biomolecule at the pH of the experiments. By comparing the results with alanine, the salting-in effect is stronger for diglycine suggesting additional specific interactions with the peptide group. A similar tendency is observed for the monovalent cations, but while for diglycine a small salting-in effect is observed, for L-alanine the effect is very small or negligible, and both Na^+ and K^+ cations even induce a small salting-out effect at higher molalities.

Conversely, all the studied salts induce a decrease on the solubility of *N*-acetylglycine, with increasing salting-out effect in the order $NH_4^+ \approx K^+ < Na^+ < Mg^{2+} \approx Ca^{2+}$. In this case, those charged complexes could not be formed due to the absence of the charged carboxylate group (Fig. S1) at a pH below 2 (observed in solutions containing Mg^{2+} or Ca^{2+}). Nevertheless, for *N*-acetylglycine, two opposite effects may arise from the absence of the COO^- and NH_3^+ charged groups, and the presence of the polar peptide bond and COOH group.

3.2. Molecular dynamics simulations

The molecular level interactions between the ions and the diglycine and *N*-acetylglycine compounds are useful to understand the specific effects of the different salts on the aqueous solubilities of the biomolecules. These interactions were analysed from the radial distribution functions (RDF) involving different groups of atoms in the diglycine and *N*-acetylglycine molecules (Fig. 2), the cations or anions of the

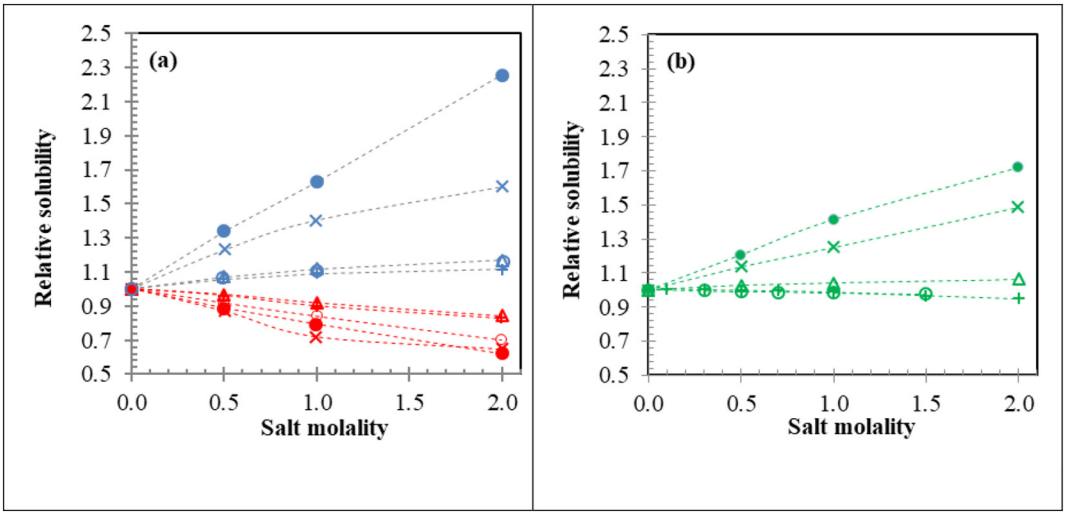

Fig. 1. Relative solubility of: (a) diglycine (blue) and *N*-acetylglycine (red), (b) alanine (green) in aqueous solutions of $CaCl_2$ (●), $MgCl_2$ (×), NH_4Cl (Δ), NaCl (○) and KCl (+), at 298.2 K. Dashed lines are plotted to guide the eye. The solubility data for glycine and *N*-acetylglycine were obtained in this work and for alanine were taken from references [1, 4, 5, 33].

salts and water. The RDFs provide a quantitative description of enhancement (values larger than 1) or depletion (values smaller than 1) of densities of species around a selected moiety.

The RDFs corresponding to the interactions between the diglycine constituting groups and the cations or anion of the NaCl, KCl, NH_4Cl, $CaCl_2$ and $MgCl_2$ salts are depicted in Fig. 3 (most important interactions) and S3 (less important interactions).

It should be noticed that the most important interactions between diglycine and the salts constituting species are those between the negatively charged carboxylate group and the cations, especially in the case of the doubly charged cations (Fig. 3a), and between the ammonium group and the chloride anion (Fig. 3b). In the case of the ammonium-chloride interactions, the RDFs for all the salts exhibit two well defined peaks at ~0.22 nm and ~0.36 nm corresponding to configurations where chloride anions interact directly with the hydrogens of the diglycine ammonium group or where the water is arranged between the chloride anion and the ammonium group, respectively. The sharp RDF peaks are also clear in the case of the interactions between CB_1 and the divalent cations. These are a result of the strong interactions between the carboxylate group and the cations (notice that the peaks in Fig. S3c appear at larger *r* values than those depicted in Fig. 3a, and again keeping their ordering due to the different sizes of the cations). Fig. 4 shows a snapshot of a configuration in the MD simulation trajectory where two chloride ions are interacting with the ammonium group of diglycine. The calculated distances between the oxygens in the carboxylate and the calcium cation are within the usual observed internuclear separations that ranges from 2.1 to 2.8 Å [34].

Based on the heights of the peaks shown in Fig. 3b, the interactions of the chloride ions with the ammonium group of diglycine are slightly more important in the cases of the solutions with NaCl, $CaCl_2$ and $MgCl_2$ salts than in the solutions with NH_4Cl and KCl. The calculated coordination numbers (error estimate <0.01) for the first peak in Fig. 3b (r = 0.285 nm) are 0.18 ($CaCl_2$), 0.17 ($MgCl_2$), 0.14 (NaCl), 0.07 (NH_4Cl) and 0.06 (KCl). The local mole fractions of the chlorides around the ammonium group of diglycine are given in Fig. S4b. Encouragingly, the ordering is well correlated with the ordering of the solubilities of diglycine in the aqueous solutions of these salts reported in Table 2.

The RDFs corresponding to interactions between the cations and the carboxylate group of diglycine (Fig. 3a) show clearly that calcium and magnesium cations are much more associated to the carboxylate oxygens atoms than NH_4^+, Na^+ and K^+ cations. The ordering dictated by the coordination numbers (values in parenthesis) after the first peak, calculated at r = 0.30 nm, is Ca^{2+} (0.66) > NH_4^+ (0.32) ≈ Mg^{2+} (0.30) > Na^+ (0.17) > K^+ (0.04), while the ordering after the second peak,

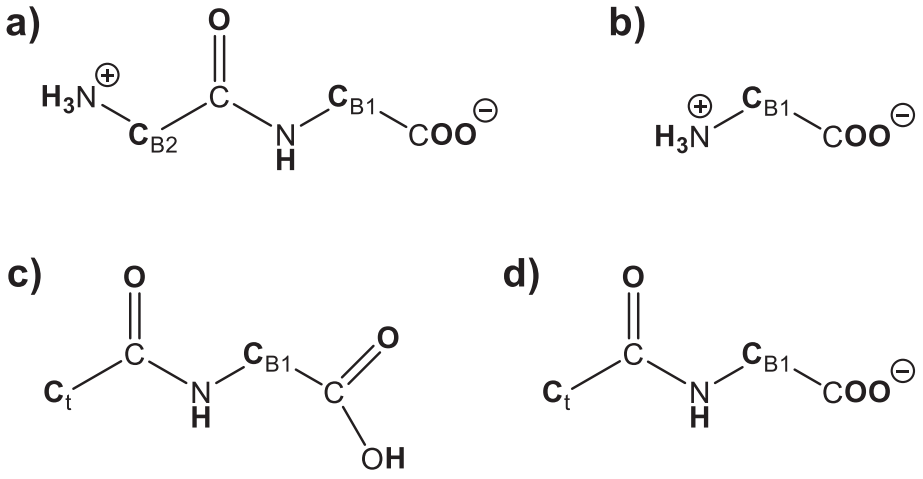

Fig. 2. Structure and atom labelling of the biomolecules studied in this work: a) zwitterionic form of diglycine, b) zwitterionic form of glycine, c) neutral form of *N*-acetylglycine and d) deprotonated form of *N*-acetylglycine. C_t stands for the terminal carbon atom of the acetyl group of *N*-acetylglycine and C_{B1} or C_{B2} for the alpha carbon atoms of the biomolecules. Hydrogen atoms directly bonded to carbon atoms were omitted for clarity and bold denotes atoms used as references for the calculation of radial distribution functions.

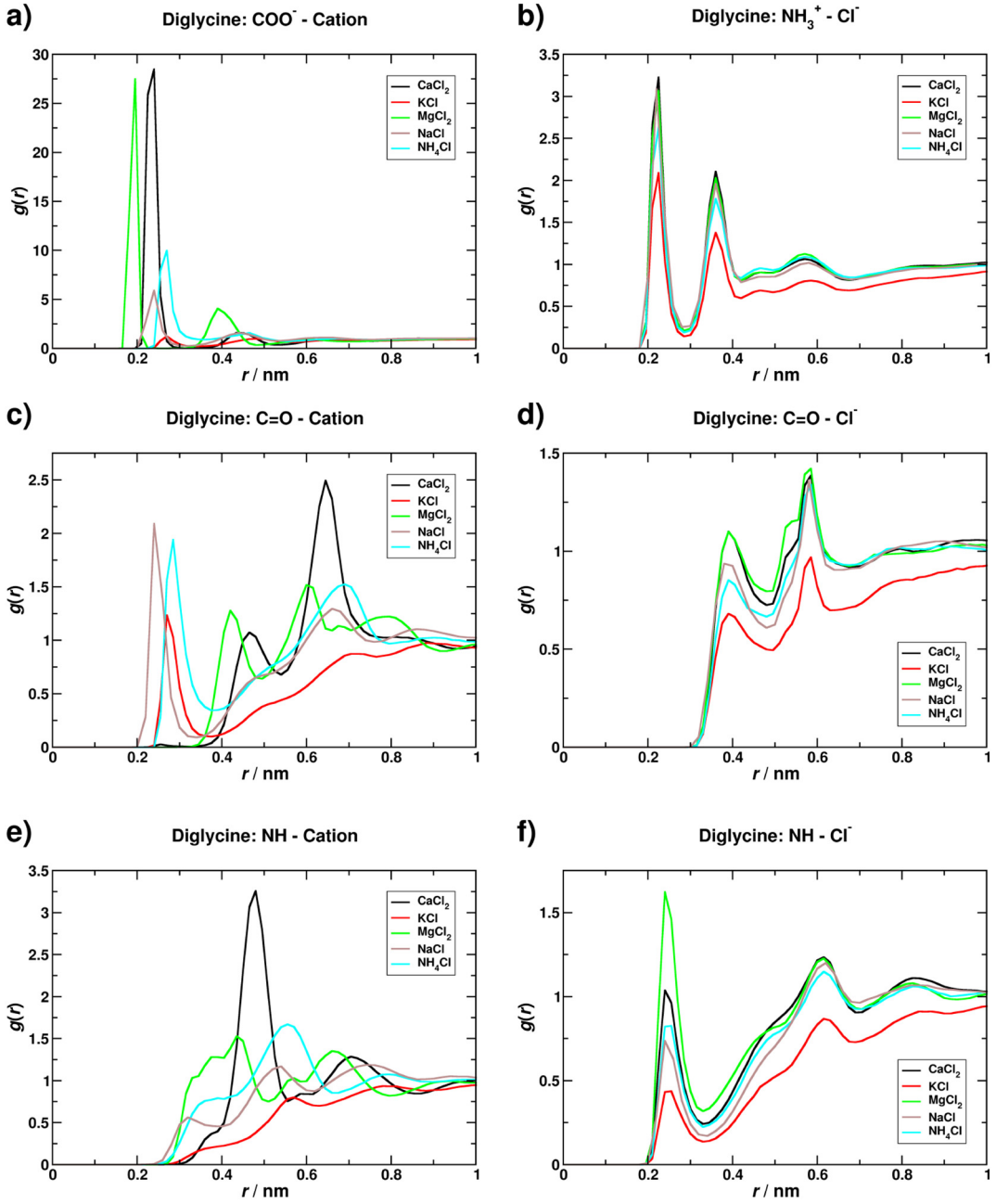

Fig. 3. Radial distribution functions of the cations (left) and the chloride anion (right) of the NaCl, KCl, NH_4Cl, $CaCl_2$ and $MgCl_2$ salts around selected groups of diglycine.

calculated at $r = 0.54$ nm, is Ca^{2+} (1.06) > Mg^{2+} (1.00) > NH_4^+ (0.96) > Na^+ (0.73) > K^+ (0.42). The local mole fractions of the cations around the carboxylate group are given in Fig. S4a. Once again, the ordering of the interactions between the cations and the carboxylate group of diglycine is well correlated with the ordering of the solubilities of diglycine in the aqueous solutions of these salts reported in Table 2. This is in good agreement with the degree of association of the cations found by Kherb et al. [35] using thermodynamic and surface spectroscopic investigations over elastin-like polypeptide containing 16 aspartic acid residues.

Considering separately both groups of cations, the divalent cations studied follow the law of matching water affinity [36], which states that oppositely charged ions (in this case carboxylate and the cations) of closer water affinity, measured comparing the hydration enthalpies of cations [37] with the corresponding value of the carboxylate, form stronger ion pairs. However, from a broader analysis over all the studied systems, that law is not obeyed for monovalent cations, as it would be expected since Na^+ presents much higher affinity to COO^-, followed by K^+ and NH_4^+.

Besides the $NH_3^+\cdots Cl^-$ and $COO^-\cdots$cation interactions, association between diglycine and the ions are also observed, albeit in a much less extension than those described above, for C═O···cation (Na^+, NH_4^+ and K^+) and NH···Cl^- interactions (panels c and f in Fig. 3, respectively), with clear peaks at r values between 0.2 and 0.3 nm. In the cases of the C═O···Ca^{2+} and C═O···Mg^{2+} interactions, the peaks in the RDFs appear at larger distances, suggesting that these associations are less relevant, which is also evident in the calculated local mole fractions shown in Fig. S4c. In fact, as can be seen in the spatial distribution functions (SDFs) for the cations and the chloride anion around diglycine shown in Fig. S5, the isosurfaces corresponding to the interactions of Ca^{2+} and Mg^{2+} with the amide's carbonyl group appear at larger distances than those corresponding to the monovalent cations. These results show that monovalent cations interact directly with the C═O group of the peptide bond while divalent cations not. This is clearly in contrast

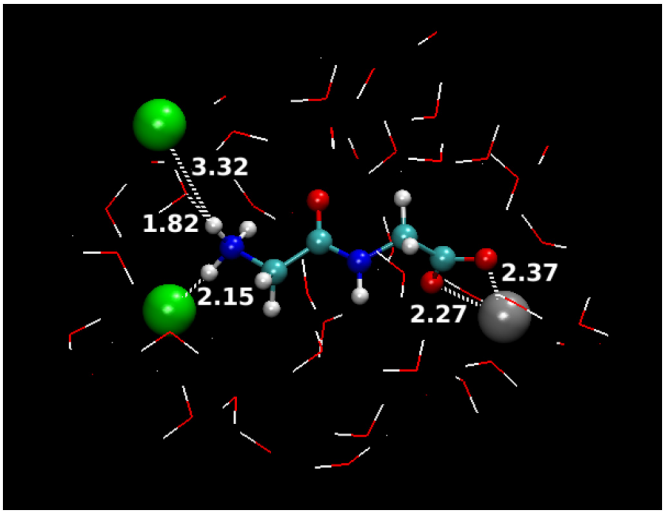

Fig. 4. Snapshot taken from the simulation of the aqueous solution of diglycine and $CaCl_2$ highlighting the atoms within a 3.5 Å radius around the center of the biomolecule. The interactions of chloride ions with the hydrogen atoms from the ammonium group of diglycine and the calcium ion with the carboxylate group are depicted in with white dashed lines. Selected values of the Cl^--$H_{ammonium}$, O_{water}-$H_{ammonium}$ and Ca^{2+}-$O_{carboxylate}$ distances are given in Å. Ball & stick representation is used for diglycine, Ca^{2+} and Cl^- species while line representation is used for water molecules. Color code for selected atoms (sphere and line representation) are: Ca, grey; Cl, green; O, red; N, blue; C, cyan; H, white.

with the results reported by some authors [38] concerning the interactions of protein backbone with cations (much weaker than with anions). Strongly hydrated cations, such as Mg^{2+} and Ca^{2+}, have a higher affinity to the carbonyl oxygen of the peptide bond than less strongly hydrated cations such as Na^+ or K^+ with lower charge density [38].

Concerning the relative strength of the ion interactions with the C═O or N—H group of the peptide bond, spectroscopic studies using butyramide to mimic the protein backbone interactions have shown that cation-amide interactions play a less important role than anion-amide interactions in the understanding the Hofmeister series [38,39], while Balos et al. [40], using dielectric relaxation spectroscopy in aqueous solution of *N*-methylacetamide (model compound), concluded that in contrast to common belief, anion-amide binding is weaker than cation-amide binding. The results found for the RDFs of C═O···cation (Fig. 3c) and N—H···anion (Fig. 3f) in diglycine do not contribute much to clarify this controversy. In fact, the RDFs for the monovalent cations show stronger correlations with the C═O group of the peptide bond, while the chloride anions in the cases of calcium or magnesium salts have higher probability of being found in the vicinity of the N—H group (see also Fig. S4c–d). Whereas the peaks present slightly higher magnitude for the monovalent cations with C═O, the N—H···anion peaks are very well defined starting for all systems at short distances.

The peaks at large *r* values in the panels of Fig. S3 corresponding to interactions between the cations or the chloride anion with the CB_1 or CB_2 carbons (e.g. the methylene groups in diglycine) are consequence of the more relevant associations described above, i.e., the cations and the chloride anion do not establish relevant interactions with these groups.

In Fig. S6 are depicted the RDFs for the interactions between the cations or the chloride ion with selected atoms from glycine (please refer to Fig. 2 for atomic labelling). Similarly to diglycine, the cations interact preferentially with the carboxylate group while the chloride ion interacts with the ammonium group of glycine; in both cases, the association between the salts ions and glycine groups varies in the order $CaCl_2$ > $MgCl_2$ > NH_4Cl > NaCl > KCl.

The RDFs corresponding to the interactions between the ions and selected atoms of neutral *N*-acetylglycine are shown in Figs. 5 and S7. In comparison with the RDFs reported for diglycine, it is observed that the solute-cation interactions are now very weak, especially in the cases of the Ca^{2+} and Mg^{2+} cations as illustrated in Figs. 5a, e and S8. Furthermore, the main interaction center with the chloride anions is that with the hydrogen atom of the carboxylic acid group. This suggests the preference of ions to remain hydrated rather than for establishing interactions with *N*-acetylglycine, which is mainly due to the more negative hydration entropies and Gibbs free energies [37,41] of Ca^{2+} and Mg^{2+} cations compared with Na^+, NH_4^+ and K^+. Notice that the relevant carboxylate-cation interactions found for glycine and diglycine are now almost absent in the case of *N*-acetylglycine (cf. compare Figs. 5e and 3a). This is a consequence of the protonation of the carboxylate group in *N*-acetylglycine, i.e., presence of a charged COO^- moiety in glycine or diglycine vs. uncharged COOH group in *N*-acetylglycine. This preferential hydration behaviour also supports the salting-out effect observed experimentally.

Concerning the relative importance of C═O and N—H of the peptide bond, it is interesting to observe that in the absence of charged groups in the *N*-acetylglycine, when compared to diglycine, the C═O···cation interactions are also less important (compare Figs. S5 and S8). Thus, monovalent cations can establish some direct interactions with the C═O group of the peptide bond (Fig. 5a) but they are less important than those in diglycine. On the contrary, the interactions with the N—H group are now absent in *N*-acetylglycine and the anion prefers to interact with the hydrogen atom in the carboxylic acid group of *N*-acetylglycine.

As it is evident from the RDFs in Fig. S9, the simulations with the 50–50% mixture of deprotonated and neutral forms of *N*-acetylglycine show that the cations preferentially interact with the negatively charged moiety (i.e., the carboxylate group) of the deprotonated *N*-acetylglycine molecules as in diglycine (Fig. 3) and glycine (Fig. S6). The pH measured in the saturated solutions of *N*-acetylglycine, however, varied between 1.1 and 3.1 (Table 3) which confirms (Fig. S1) that *N*-acetylglycine is almost completely in the neutral form, but MD simulations suggest that upon increasing the pH, divalent cations (in particular) can enhance greatly the solubility of the *N*-acetylglycine.

4. Conclusions

New experimental data on the salt effect on the solubility of diglycine or *N*-acetylglycine in water have been measured at 298.2 K. The two biomolecules show an opposite behaviour. The solubility of *N*-acetylglycine decreases with the salt concentration increase, while the solubility of diglycine increases. The salting-in magnitude for diglycine is much more evident for salts with divalent cations than using the monovalent cation salts.

Molecular dynamics simulations were performed to obtain further insight into the molecular-level interactions that control the solubilities of diglycine and *N*-acetylglycine experimentally observed in aqueous solutions of NaCl, KCl, NH_4Cl, $CaCl_2$ or $MgCl_2$. The salts containing divalent cations promote a pronounced salting-in for diglycine, and also the highest salting-out effect for *N*-acetylglycine. Based on the results from the MD simulations, the salting-in effects of diglycine were interpreted as strong interactions of the cations with the carboxylate group of diglycine, especially in the case of the divalent cations, in agreement with previous studies with amino acids. All the studied salts induce salting-out of *N*-acetylglycine in aqueous saline solutions. Since at the low pH of these solutions the compound is mostly in its neutral form, MD simulations show that the most relevant interactions were those between the chloride anion and the hydrogen atom of the carboxylic group and between the C═O of the peptide bond and the cation, which can be correlated to the weaker salting-out effect of the monovalent cations when compared to the divalent ones.

Even if some trends were identified on the relevance of the interaction between the C═O group of the peptide bond and the cations, the molecular dynamics and experimental solubility studies should be

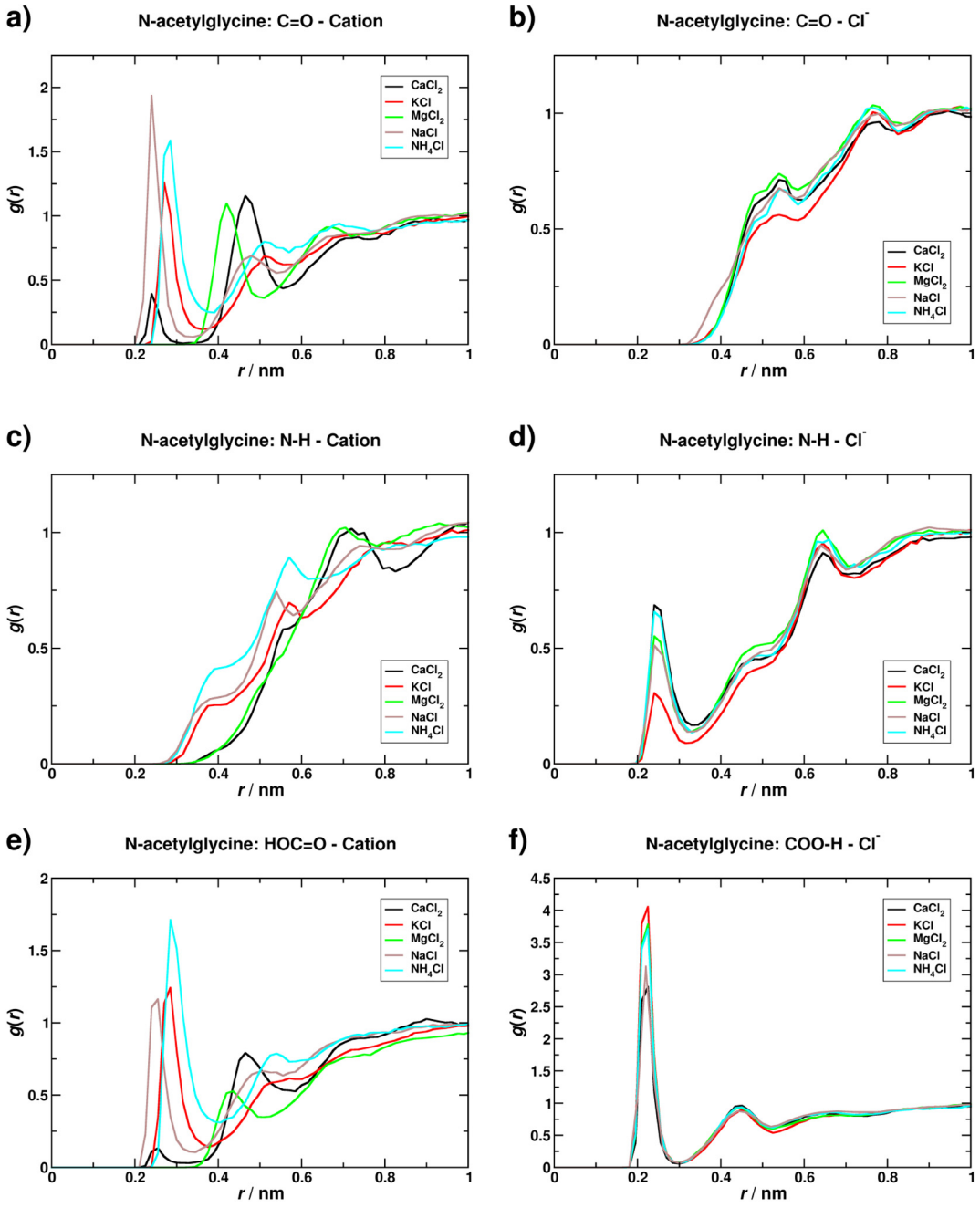

Fig. 5. Radial distribution functions of the cations (left) and the chloride anion (right) of the NaCl, KCl, NH_4Cl, $CaCl_2$ and $MgCl_2$ salts around selected groups of neutral *N*-acetylglycine.

extended to other salts with the same set of cations, but different anions. These two biomolecules were used as model compounds to understand more complex systems, such as systems containing proteins, where ion-ion interactions at the biomolecule surfaces and in the surrounding aqueous medium play an important role and, in this way, must be also extended to larger polypeptides showing different functionalities.

CRediT authorship contribution statement

Germán Pérez-Sánchez: Investigation, Writing - original draft. **Yoselyn S. Santos:** Investigation. **Olga Ferreira:** Investigation, Supervision, Data curation, Writing - original draft. **João A.P. Coutinho:** Supervision, Validation. **José R.B. Gomes:** Conceptualization, Supervision, Writing - review & editing. **Simão P. Pinho:** Conceptualization, Supervision, Validation, Writing - review & editing.

Declaration of competing interest

The authors declare that they have no known competing financial interests or personal relationships that could have appeared to influence the work reported in this paper.

Acknowledgments

We acknowledge the support of the project "AIProcMat@N2020 - Advanced Industrial Processes and Materials for a Sustainable Northern Region of Portugal 2020", with the reference NORTE-01-0145-FEDER-000006, supported by Norte Portugal Regional Operational Programme (NORTE 2020), under the Portugal 2020 Partnership Agreement, through the European Regional Development Fund (ERDF); Associate Laboratory LSRE-LCM - UID/EQU/50020/2019 - funded by national funds through FCT/MCTES (PIDDAC), and CIMO-Mountain Research

Center, UIDB/00690/2020. This work received also funds from the Fundação para a Ciência e a Tecnologia (FCT) through project CICECO (POCI-01-0145-FEDER-007679 and UID/CTM/50011/2020), and Programa Investigador FCT, financed by national funds through the FCT/MEC and co-financed by FEDER under the PT2020 Partnership Agreement.

Appendix A. Supplementary data

Supplementary data to this article can be found online at https://doi.org/10.1016/j.molliq.2020.113044.

References

[1] L. Ferreira, E. Macedo, S. Pinho, Effect of KCl and Na2SO4 on the solubility of glycine and DL-alanine in water at 298.15 K, Ind. Eng. Chem. Res. 44 (2005) 8892–8898.
[2] L.A. Ferreira, E.A. Macedo, S.P. Pinho, The effect of ammonium sulfate on the solubility of amino acids in water at (298.15 and 323.15)K, J. Chem. Thermodyn. 41 (2009) 193–196.
[3] L.A. Ferreira, E.A. Macedo, S.P. Pinho, KCl effect on the solubility of five different amino acids in water, Fluid Phase Equilib. 255 (2007) 131–137.
[4] L.I.N. Tomé, C.S.R. Sousa, J.R.B. Gomes, O. Ferreira, J.A.P. Coutinho, S.P. Pinho, Understanding the cation specific effects on the aqueous solubility of amino acids: from mono to polyvalent cations, RSC Adv. 5 (2015) 15024–15034.
[5] L.I.N. Tomé, S. Pinho, M. Jorge, J.R.B. Gomes, J.A.P. Coutinho, Salting-in with a salting-out agent: explaining the cation specific effects on the aqueous solubility of amino acids, J. Phys. Chem. 117 (2013) 6116–6128.
[6] D.R. Robinson, W.P. Jencks, The effect of concentrated salt solutions on the activity coefficient of acetyltetraglycine ethyl ester, J. Am. Chem. Soc. 87 (1965) 2470–2479.
[7] P.K. Nandi, D.R. Robinson, Effects of salts on the free energies of nonpolar groups in model peptides, J. Am. Chem. Soc. 94 (1972) 1308–1315.
[8] P.K. Nandi, D.R. Robinson, Effects of salts on the free energy of the peptide group, J. Am. Chem. Soc. 94 (1972) 1299–1308.
[9] J. Paterová, K.B. Rembert, J. Heyda, Y. Kurra, H.I. Okur, W.R. Liu, C. Hilty, P.S. Cremer, P. Jungwirth, Reversal of the hofmeister series: specific ion effects on peptides, J. Phys. Chem. B 117 (2013) 8150–8158.
[10] H. Talukdar, S. Rudra, K.K. Kundu, Thermodynamics of transfer of glycine, diglycine, and triglycine from water to aqueous solutions of urea, glycerol, and sodium nitrate, Can. J. Chem. 66 (1988) 461–468.
[11] M.P. Breil, J.M. Mollerup, E.S.J. Rudolph, M. Ottens, L.A.M. Van Der Wielen, Densities and solubilities of glycylglycine and glycyl-L-alanine in aqueous electrolyte solutions, Fluid Phase Equilib. 215 (2004) 221–225.
[12] J. Lu, X.J. Wang, X. Yang, C.B. Ching, Solubilities of glycine and its oligopeptides in aqueous solutions, J. Chem. Eng. Data 51 (2006) 1593–1596.
[13] P. Venkatesu, M.-J. Lee, H.-M. Lin, Transfer free energies of peptide backbone unit from water to aqueous electrolyte solutions at 298.15K, Biochem. Eng. J. 32 (2006) 157–170.
[14] B.R. Brooks, C.L. Brooks, A.D. MacKerell, L. Nilsson, R.J. Petrella, B. Roux, Y. Won, G. Archontis, C. Bartels, S. Boresch, A. Caflisch, L. Caves, Q. Cui, A.R. Dinner, M. Feig, S. Fischer, J. Gao, M. Hodoscek, W. Im, K. Kuczera, T. Lazaridis, J. Ma, V. Ovchinnikov, E. Paci, R.W. Pastor, C.B. Post, J.Z. Pu, M. Schaefer, B. Tidor, R.M. Venable, H.L. Woodcock, X. Wu, W. Yang, D.M. York, M. Karplus, CHARMM: the biomolecular simulation program, J. Comput. Chem. 30 (2009) 1545–1614.
[15] S. Pronk, S. Páll, R. Schulz, P. Larsson, P. Bjelkmar, R. Apostolov, M.R. Shirts, J.C. Smith, P.M. Kasson, D. Van Der Spoel, B. Hess, E. Lindahl, GROMACS 4.5: a high-throughput and highly parallel open source molecular simulation toolkit, Bioinformatics 29 (2013) 845–854.
[16] M.S. Santosh, A.P. Lyubartsev, A.A. Mirzoev, D.K. Bhat, Molecular dynamics investigation of dipeptide-transition metal salts in aqueous solutions, J. Phys. Chem. B 114 (2010) 16632–16640.
[17] K. Kwac, K.K. Lee, J.B. Han, K.I. Oh, M. Cho, Classical and quantum mechanical/molecular mechanical molecular dynamics simulations of alanine dipeptide in water: comparisons with IR and vibrational circular dichroism spectra, J. Chem. Phys. 128 (2008), 105106. .
[18] L. Ma, L. Pegram, M.T. Record, Q. Cui, Preferential interactions between small solutes and the protein backbone: a computational analysis, Biochemistry 49 (2010) 1954–1962.
[19] L.I.N. Tomé, M. Jorge, J.R.B. Gomes, J.A.P. Coutinho, Toward an understanding of the aqueous solubility of amino acids in the presence of salts: a molecular dynamics simulation study, J. Phys. Chem. B 114 (2010) 16450–16459.
[20] L.I.N. Tomé, M. Jorge, J.R.B. Gomes, J.A.P. Coutinho, Molecular dynamics simulation studies of the interactions between ionic liquids and amino acids in aqueous solution, J. Phys. Chem. B 116 (2012) 1831–1842.
[21] F. Hofmeister, Zur Lehre von der Wirkung der Salze - Zweite Mittheilung, Arch. Exp. Pathol. Pharmakol. 24 (1888) 247–260.
[22] S. Nosé, A molecular dynamics method for simulations in the canonical ensemble, Mol. Phys. 52 (1984) 255–268.
[23] W.G. Hoover, Canonical dynamics: equilibrium phase-space distributions, Phys. Rev. A 31 (1985) 1695–1697.
[24] M. Parrinello, A. Rahman, Polymorphic transitions in single crystals: a new molecular dynamics method, J. Appl. Phys. 52 (1981) 7182–7190.
[25] R. Hockney, S. Goel, J. Eastwood, Quiet high-resolution computer models of a plasma, J. Comput. Phys. 14 (1974) 148–158.
[26] U. Essmann, L. Perera, M.L. Berkowitz, T. Darden, H. Lee, L.G. Pedersen, A smooth particle mesh Ewald method, J. Chem. Phys. 103 (1995) 8577–8593.
[27] B. Hess, H. Bekker, H.J.C. Berendsen, J.G.E.M. Fraaije, LINCS: a linear constraint solver for molecular simulations, J. Comput. Chem. 18 (1997) 1463–1472.
[28] H.J.C. Berendsen, J.R. Grigera, T.P. Straatsma, The missing term in effective pair potentials, J. Phys. Chem. 91 (1987) 6269–6271.
[29] W.L. Jorgensen, D.S. Maxwell, J. Tirado-Rives, Development and testing of the OPLS all-atom force field on conformational energetics and properties of organic liquids, J. Am. Chem. Soc. 118 (1996) 11225–11236.
[30] G.A. Kaminski, R.A. Friesner, J. Tirado-Rives, W.L. Jorgensen, Evaluation and reparametrization of the OPLS-AA force field for proteins via comparison with accurate quantum chemical calculations on peptides, J. Phys. Chem. B 105 (2001) 6474–6487.
[31] J. Åqvist, Ion-water interaction potentials derived from free energy perturbation simulations, J. Phys. Chem. 94 (1990) 8021–8024.
[32] J. Heyda, T. Hrobárik, P. Jungwirth, Ion-specific interactions between halides and basic amino acids in water, J. Phys. Chem. A 113 (2009) 1969–1975.
[33] M.K. Khoshkbarchi, J.H. Vera, Effect of NaCl and KCl on the solubility of amino acids in aqueous solutions at 298.2 K: measurements and modeling, Ind. Eng. Chem. Res. Eng. Chem. Res. 36 (1997) 2445–2451.
[34] T. Dudev, C. Lim, Principles governing mg, Ca, and Zn binding and selectivity in proteins, Chem. Rev. 103 (2003) 773–788.
[35] J. Kherb, S.C. Flores, P.S. Cremer, Role of carboxylate side chains in the cation Hofmeister series, J. Phys. Chem. B 116 (2012) 7389–7397.
[36] K. Collins, Ions from the Hofmeister series and osmolytes: effects on proteins in solution and in the crystallization process, Methods 34 (2004) 300–311.
[37] Y. Marcus, Thermodynamics of solvation of ions. Part 5.—Gibbs free energy of hydration at 298.15 K, J. Chem. Soc. Faraday Trans. 87 (1991) 2995–2999.
[38] P. Jungwirth, P.S. Cremer, Beyond Hofmeister, Nat. Chem. 6 (2014) 261–263.
[39] H.I. Okur, J. Kherb, P.S. Cremer, Cations bind only weakly to amides in aqueous solutions, J. Am. Chem. Soc. 135 (2013) 5062–5067.
[40] V. Balos, M. Bonn, J. Hunger, Anionic and cationic Hofmeister effects are non-additive for guanidinium salts, Phys. Chem. Chem. Phys. 19 (2017) 9724–9728.
[41] Y. Marcus, A. Loewenschuss, Chapter 4. Standard entropies of hydration of ions, Annu. Reports Sect. 'C' (Physical Chem), vol. 81, 1984, p. 81.